Nonequilibrium effects and baryogenesis

Yeo-Yie Charng,[1,*] Da-Shin Lee,[2,3,†] Chung Ngoc Leung,[4,‡] and Kin-Wang Ng[1,§]

[1]*Institute of Physics, Academia Sinica, Taipei, Taiwan 115, Republic of China*
[2]*Department of Physics, National Dong Hwa University, Hua-Lien, Taiwan 974, Republic of China*
[3]*The Theory Group, Blackett Laboratory, Imperial College, London SW7 2BZ, United Kingdom*
[4]*Department of Physics and Astronomy, University of Delaware, Newark, Delaware 19716, USA*

(Received 30 June 2005; published 22 December 2005)

Possible effects due to nonequilibrium dynamics in the Affleck-Dine mechanism of baryogenesis are examined. Using the closed-time-path formalism, the quantum fluctuation and the backreaction of the Affleck-Dine scalar field are incorporated self-consistently into the dynamical equations of the system by invoking a nonperturbative Hartree approximation. It is found that such nonequilibrium effects can significantly affect the amount of baryon asymmetry that can be generated. In particular, it is possible to generate the observed baryon asymmetry with suitable initial conditions. The methodology described in this paper as well as some of the results obtained are quite general, and can be applied to any complex scalar field in a cosmological background.

DOI: 10.1103/PhysRevD.72.123517 PACS numbers: 98.80.Qc, 03.70.+k, 98.80.Cq

I. INTRODUCTION

It is evident that no concentration of antimatter exists within the Solar system and the Milky Way. The absence of annihilation radiation from the Virgo cluster indicates that antimatter can hardly be found within a 20 Mpc scale. A study of the contribution of annihilation radiation near the matter-antimatter boundaries to the cosmic diffuse gamma-ray background virtually excludes domains of antimatter in the visible Universe [1].

Direct observations of luminous matter show that baryons constitute about a few percents of the total mass of the Universe. This gives a value of order 10^{-10} for n_B/s, the ratio of the baryon-number density to the entropy density. Precise measurements of the abundance of primordial light elements predicted in big-bang nucleosynthesis combined with the cosmic microwave background experiments restrict this ratio in the range $n_B/s \simeq (5-10)\times 10^{-11}$ [2].

Many scenarios for baryon production in the early Universe have been proposed to explain this small baryon asymmetry, such as baryogenesis in grand unified theories, electroweak baryogenesis, leptogenesis, and Affleck-Dine (AD) baryogenesis [3]. Affleck and Dine [4] proposed a mechanism of baryogenesis in supersymmetric models in which scalar quark and lepton fields obtain large vacuum expectation values along flat directions of the scalar potential. These coherent scalars or the condensate start to oscillate at a temperature of order 10 TeV when supersymmetry-breaking effects start to become important, and a net baryon number is developed and stored in the oscillating fields provided that C and CP symmetries are also violated. Subsequently, the scalar quark and lepton fields decay and produce a baryon asymmetry. In fact, the AD mechanism is too efficient and the resulting baryon asymmetry is usually too large. Several dilution processes have been considered to reduce the large baryon asymmetry to the observed value. They involve either introducing additional entropy releases after baryogenesis (e.g., by the decays of the inflaton [5], massive field fluctuations [6], or the dilaton [7]) or reducing the baryon production by invoking nonrenormalizable terms [8]. In all of these studies, the scalar fermion fields have been treated as classical fields and obey the classical equations of motion. In this paper, we will be concerned with quantum fluctuations created from the dynamics of the Affleck-Dine scalar field and its backreaction effects. In particular, we study how these nonequilibrium processes affect the baryon production in the AD mechanism.

It has been proposed that in a certain AD flat direction the condensate is not the state of lowest energy but fragments to form metastable or stable Q-balls, depending on the shape of the radiative correction to the flat direction [3]. For instance, this occurs along the flat direction with large mixtures of scalar top quark and light gaugino masses or in the H_uL-direction. In this paper we estimate the baryon asymmetry assuming that the AD condensate does not lead to this type of Q-ball formation. Our presentation is organized as follows. The model of Affleck-Dine baryogenesis is described in Sec. II. We introduce the method of nonequilibrium field theory in Sec. III. It is then applied to the Affleck-Dine model in Sec. IV. We show in Sec. V how to incorporate nonequilibrium effects in the calculation of the baryon asymmetry, and present the results of our numerical calculation and discuss their implications in Sec. VI. Our conclusions are offered in Sec. VII.

II. AFFLECK-DINE BARYOGENESIS

Affleck and Dine [4] have shown that, in a supersymmetric SU(5) grand unified model, there is a flat direction

*Electronic address: charng@phys.sinica.edu.tw
†Electronic address: dslee@mail.ndhu.edu.tw
corresponding author.
‡Electronic address: leung@physics.udel.edu
§Electronic address: nkw@phys.sinica.edu.tw

in the low-energy effective potential for the following set of vacuum states of the up ($\tilde{u}$), strange ($\tilde{s}$), and bottom ($\tilde{b}$) squark fields as well as the scalar muon field ($\tilde{\mu}$):

$$\begin{aligned} &\langle \tilde{u}_3^c \rangle = a, \qquad \langle \tilde{u}_1 \rangle = v; \qquad \langle \tilde{s}_2^c \rangle = a, \\ &\langle \tilde{\mu} \rangle = v; \qquad \langle \tilde{b}_1^c \rangle = e^{i\xi}\sqrt{|v|^2 + |a|^2}, \end{aligned} \tag{1}$$

with all other fields having vanishing vacuum expectation values. Here the superscript c denotes charge conjugation, the subscripts denote color indices, a and v are arbitrary complex numbers, and ξ is real. A large baryon asymmetry can be generated by the decays of the condensate associated with these vacuum expectation values via baryon-number violating dimension-four scalar couplings which appear after supersymmetry has been broken. To illustrate how the mechanism works, Affleck and Dine considered a toy model with a single complex scalar field Φ described by the Lagrangian density

$$\mathcal{L} = (\partial_\mu \Phi^\dagger)(\partial^\mu \Phi) - m_\Phi^2 \Phi^\dagger \Phi - i\lambda(\Phi^4 - \Phi^{\dagger 4}), \tag{2}$$

which contains the mass term with $m_\Phi^2 = M_S^2$ and the baryon-number violating coupling, $\lambda \sim \epsilon M_S^2/M_G^2$, where M_S is the effective supersymmetry-breaking scale, ϵ is a real parameter characterizing CP violation, and M_G is the grand unification scale. For small Φ, the theory has an approximately conserved current

$$j_\mu = i(\Phi^\dagger \partial_\mu \Phi - (\partial_\mu \Phi^\dagger)\Phi) \tag{3}$$

due to the approximate global $U(1)$ symmetry: $\Phi \rightarrow e^{i\theta}\Phi$. The corresponding charge will be referred to as the baryon number (this will be the case if, for example, Φ represents a scalar quark field).

Classically, in an expanding universe, Φ obeys the equation of motion

$$\frac{d^2\Phi}{dt^2} + 3H\frac{d\Phi}{dt} + m_\Phi^2 \Phi = 4i\lambda \Phi^{\dagger 3}, \tag{4}$$

where H is the Hubble parameter. With the initial conditions at $t = t_0$:

$$\Phi|_{t=t_0} = i\Phi_0 \quad \text{and} \quad \dot{\Phi}|_{t=t_0} = 0, \tag{5}$$

where Φ_0 is real and $\dot{\Phi} = d\Phi/dt$, it was found that the baryon number per particle at large times ($t \gg m_\Phi^{-1}$) in either a matter-dominated or a radiation-dominated universe is given by

$$r \simeq \lambda \Phi_0^2/m_\Phi^2. \tag{6}$$

Assuming $m_\Phi^2 = M_S^2$ and $\lambda = \epsilon M_S^2/M_G^2$, we have $r \simeq \epsilon \Phi_0^2/M_G^2$, which can easily provide a large initial n_B/s and thus dilution processes have to be introduced to reduce it to the observed value. For example, taking $\epsilon = 10^{-3}$, $M_S = 10^{-16} M_P$, $M_G = 10^{-1} M_P$, and $\Phi_0^2 = 10^{-3} M_P^2$, where M_P is the Planck mass, we find $\lambda = 10^{-33}$ and $r \simeq 10^{-4}$. Note that the decay width of the condensate can be estimated as $\Gamma_\Phi \sim (\alpha_s/\pi)^2 m_\Phi^3/|\Phi|^2$ [4], which is typically much smaller than the frequency of the oscillating scalar fields, i.e., $\Gamma_\Phi \ll m_\Phi$. Therefore, a net baryon number is developed and gets saturated in the oscillating scalar quark and lepton fields before they decay and produce a baryon asymmetry.

The above consideration did not take into account the fact that a dynamical background field could generate quantum fluctuations which could in turn influence its evolution [9–12]. Substantial quantum fluctuations from the vacuum state may lead to a value of the generated baryon-number density quite different from that obtained from purely classical arguments. In the following sections, we will study how the quantum fluctuation of the dynamical Φ field and the backreaction on its evolution will affect the ratio r for the model of Eq. (2). Nonperturbative Hartree factorizations will be implemented along with the method of nonequilibrium quantum field theory to self-consistently take account of quantum fluctuations and back-reaction effects on the background field. To be completely general, we will not fix the values of m_Φ, λ, and Φ_0, leaving them as free parameters.

III. NONEQUILIBRIUM QUANTUM FIELD THEORY

Before we discuss the Affleck-Dine baryogenesis, let us review the field theoretical methods for treating the quantum fluctuation and backreaction of a dynamical quantum field. The basic methods for studying nonequilibrium phenomena were developed many years ago by Schwinger and Keldysh [13]. In nonequilibrium situations we are interested in obtaining the equations of motion for the expectation values and correlation functions of the quantum fields in an evolving quantum state or density matrix. This is accomplished by tracking the time evolution of the density matrix, which corresponds to an initial valued problem for the Liouville equation.

In the Schrödinger picture the evolution of the density matrix ρ is determined by

$$\rho(t) = U(t, t_0)\rho(t_0)U^{-1}(t, t_0), \tag{7}$$

where $U(t, t_0)$ is the time evolution operator:

$$U(t, t_0) = \mathcal{T} \exp\left[-i \int_{t_0}^{t} dt' H(t') \right] \tag{8}$$

for a time-dependent Hamiltonian H. The symbol $\mathcal{T}$ means to take the time-ordered product. The expectation value of an operator $\mathcal{O}$ in the Schrödinger picture is given by

$$\langle \mathcal{O} \rangle(t) = \frac{\mathrm{Tr}[U(t, t_0)\rho(t_0)U^{-1}(t, t_0)\mathcal{O}]}{\mathrm{Tr}[\rho(t_0)]}, \tag{9}$$

and thus can be determined once the initial density matrix $\rho(t_0)$ is specified.

Consider the case in which the initial density matrix describes a system in equilibrium. When a perturbation is switched on at time t_0, the resulting time-dependent Hamiltonian can drive the initial state out of equilibrium. Just as in the usual perturbation theory, we write $H = H_0 + H_{\rm int}$, where H_0 is the unperturbed quadratic Hamiltonian and $H_{\rm int}$ stands for the perturbations. For technical convenience of treating this initial valued problem, we can model the dynamics by the following Hamiltonian:

$$H(t) = \Theta(t_0 - t)H_0(t_0) + \Theta(t - t_0)[H_0(t) + H_{\rm int}(t)], \tag{10}$$

where $\Theta(t - t_0)$ is the Heaviside step function. For $t < t_0$, the unperturbed Hamiltonian $H_0(t_0)$ is fixed at time t_0 from which we can specify the initial thermal state of the system, and for $t > t_0$, the perturbation is switched on in $H_{\rm int}$. Before the perturbation is switched on, the system is assumed to be in equilibrium at a temperature $T = 1/\beta$ and is described by the initial density matrix

$$\rho(t_0) = \exp[-\beta H_0(t_0)]. \tag{11}$$

The zero temperature limit for an initial vacuum state can be obtained by taking $T \to 0$, as we shall consider later.

Notice that the initial density matrix can be expressed in terms of the time evolution operator along imaginary time in the distant past: $\rho(t_0) = U(-\infty - i\beta, -\infty)$. This allows us to write the expectation value in Eq. (9) as

$$\langle \mathcal{O} \rangle(t) = \frac{\mathrm{Tr}[U(-\infty - i\beta, -\infty)U^{-1}(t, -\infty)\mathcal{O}U(t, -\infty)]}{\mathrm{Tr}[U(-\infty - i\beta, -\infty)]}, \tag{12}$$

where we have inserted $U(t_0, -\infty)U^{-1}(t_0, -\infty) = 1$ to the right of $\rho(t_0)$ in the numerator, commuted $U(t_0, -\infty)$ with $\rho(t_0)$, and used the following composition property of the evolution operator: $U^{-1}(t_0, -\infty)U^{-1}(t, t_0) = [U(t, t_0)U(t_0, -\infty)]^{-1} = U^{-1}(t, -\infty)$. Another insertion of $1 = U^{-1}(\infty, t)U(\infty, t)$ yields

$$\langle \mathcal{O} \rangle(t) = \frac{\mathrm{Tr}[U(-\infty - i\beta, -\infty)U^{-1}(\infty, -\infty)U(\infty, t)\mathcal{O}U(t, -\infty)]}{\mathrm{Tr}[U(-\infty - i\beta, -\infty)]}. \tag{13}$$

Although not apparent from the above expression, the time-dependent expectation value for $\mathcal{O}$ depends implicitly on t_0 through the perturbation $H_{\rm int}$ which is switched on at time t_0. Because there are both forward and backward [given by $U^{-1}(\infty, -\infty)$] time evolutions, and because the initial density matrix is written as the time evolution operator along imaginary time, one is led to consider the following generating functional

$$\mathcal{Z}[j^+, j^-] = \mathrm{Tr}[U(-\infty - i\beta, -\infty)U(-\infty, \infty, j^-) \times U(\infty, -\infty, j^+)] \tag{14}$$

for deriving the nonequilibrium equations of motion for the expectation values and correlation functions of the quantum fields.

In anticipation of the subsequent application to the Affleck-Dine model (2) for baryogenesis, let us consider the case of a scalar field φ as an example. In this case the generating functional above has the following path-integral representation

$$\mathcal{Z}[j^+, j^-] = \int d\varphi d\varphi_1 d\varphi_2 \int \mathcal{D}\varphi^+ \mathcal{D}\varphi^- \mathcal{D}\varphi^\beta \exp\left(i \int_{-\infty}^{\infty} dt \int d^3\mathbf{x}\{\mathcal{L}[\varphi^+] + j^+\varphi^+\}\right) \times \exp\left(-i \int_{-\infty}^{\infty} dt \int d^3\mathbf{x}\{\mathcal{L}[\varphi^-] + j^-\varphi^-\}\right) \exp\left(i \int_{-\infty}^{-\infty - i\beta} dt \int d^3\mathbf{x}\{\mathcal{L}_0[\varphi^\beta]\}\right) \tag{15}$$

with the boundary conditions: $\varphi^+(\mathbf{x}, -\infty) = \varphi^\beta(\mathbf{x}, -\infty - i\beta) = \varphi(\mathbf{x})$, $\varphi^+(\mathbf{x}, \infty) = \varphi^-(\mathbf{x}, \infty) = \varphi_1(\mathbf{x})$, and $\varphi^-(\mathbf{x}, -\infty) = \varphi^\beta(\mathbf{x}, -\infty) = \varphi_2(\mathbf{x})$. The path integrals represented by the φ^+ and φ^- fields correspond to the forward and backward time evolution, respectively, while the one described by the φ^β field corresponds to the time evolution along the path parallel to the imaginary time axis. The boundary conditions are in fact a result of the trace as well as the bosonic nature of the operators. Notice that the path integral corresponding to evolution in imaginary time involves only the unperturbed quadratic Lagrangian $\mathcal{L}_0$ [see Eq. (10)], while the other path integrals involve the full Lagrangian $\mathcal{L} = \mathcal{L}_0 + \mathcal{L}_{\rm int}$, where $\mathcal{L}_{\rm int}$ stands for the interaction Lagrangian that will be treated as a perturbation.

The introduction of sources in Eq. (15) allows one to obtain expectation values involving the quantum field operators by taking functional derivatives with respect to the sources as follows:

$$\varphi^+ \to -i\frac{\delta}{\delta j^+}, \qquad \varphi^- \to i\frac{\delta}{\delta j^-}, \tag{16}$$

and then setting the sources to zero in the end. In fact, various Green functions can be obtained by taking functional derivatives of the generating function with respect to the appropriate sources. For instance, functional differentiation with respect to the sources j^+ and j^- can generate the time-ordered and anti-time-ordered Green functions, respectively.

As for computing the real-time correlation functions of interest, there is clearly no need to introduce any source along the path parallel to the imaginary time axis since the Lagrangian along this path involves only its unperturbed part $\mathcal{L}_0$. In the Schrödinger picture, the ensemble average we implement corresponds to an initial density matrix describing a state of thermal equilibrium with respect to the unperturbed Hamiltonian. Path integrals over $\mathcal{L}_0$ can be carried out exactly and we can obtain the generating functional in terms of the nonequilibrium propagators. The temperature dependence enters through the boundary conditions on the nonequilibrium propagators as we shall see later. Thus, the relevant generating functional for computing real-time correlation functions can be obtained as

$$\mathcal{Z}[j^+, j^-] = \exp\left\{ i \int d^4x \left(\mathcal{L}_{\rm int}\left[-i\frac{\delta}{\delta j^+} \right] - \mathcal{L}_{\rm int}\left[i\frac{\delta}{\delta j^-} \right] \right) \right\} \exp\left\{ -\frac{1}{2} \int d^4x \int d^4x' [j^+(x) G^{++}(x, x') j^+(x') - j^+(x) G^{+-}(x, x') j^-(x') - j^-(x) G^{-+}(x, x') j^+(x') + j^-(x) G^{--}(x, x') j^-(x')] \right\}, \tag{17}$$

where the nonequilibrium propagators corresponding to the forward and backward time branches are given by

$$\begin{aligned} G^{++}(\mathbf{x}, \mathbf{x}'; t, t') &= \langle \varphi^+(\mathbf{x}, t) \varphi^+(\mathbf{x}', t') \rangle = G^>(\mathbf{x}, \mathbf{x}'; t, t') \Theta(t - t') + G^<(\mathbf{x}, \mathbf{x}'; t, t') \Theta(t' - t), \\ G^{--}(\mathbf{x}, \mathbf{x}'; t, t') &= \langle \varphi^-(\mathbf{x}, t) \varphi^-(\mathbf{x}', t') \rangle = G^>(\mathbf{x}, \mathbf{x}'; t, t') \Theta(t' - t) + G^<(\mathbf{x}, \mathbf{x}'; t, t') \Theta(t - t'), \\ G^{+-}(\mathbf{x}, \mathbf{x}'; t, t') &= \langle \varphi^+(\mathbf{x}, t) \varphi^-(\mathbf{x}', t') \rangle = G^<(\mathbf{x}, \mathbf{x}'; t, t') = \langle \varphi(\mathbf{x}', t') \varphi(\mathbf{x}, t) \rangle, \\ G^{-+}(\mathbf{x}, \mathbf{x}'; t, t') &= \langle \varphi^-(\mathbf{x}, t) \varphi^+(\mathbf{x}', t') \rangle = G^>(\mathbf{x}, \mathbf{x}'; t, t') = \langle \varphi(\mathbf{x}, t) \varphi(\mathbf{x}', t') \rangle. \end{aligned} \tag{18}$$

Since time translational invariance is lost for a system that is out of equilibrium, the Green functions defined above will in general depend on the time t and t' separately.

The functions $G^>$ and $G^<$ can be obtained from computing the 2-point correlation functions of the quantum field φ, which can be expressed in terms of the usual creation and annihilation operators with mode functions that are solutions to the homogeneous equations of motion for the quadratic Lagrangian $\mathcal{L}_0$. The explicit derivation for them will be shown in the next section. As a result of the assumed initial thermal state mentioned above, they obey the boundary condition

$$G^<(\mathbf{x}, \mathbf{x}'; -\infty, t') = G^>(\mathbf{x}, \mathbf{x}'; -\infty - i\beta, t'), \tag{19}$$

which corresponds to the Kubo-Martin-Schwinger (KMS) condition at a large negative time before the pertubation is switched on [14].

In summary, the generating functional (17) can be used to obtain the Feynman rules that define the perturbative expansion for weak couplings. There are four sets of nonequilibrium propagators in the forms given in Eq. (18). Two sets of interaction vertices defined by the interaction Lagrangian $\mathcal{L}_{\rm int}$ involve fields in the forward branch and those in the backward branch. Notice that there exists a relative minus sign difference between these two types of vertices. The calculation of the combinatorial factors is the same as in the usual quantum field theory. This constitutes the basic tool for our studies.

IV. COMPLEX SCALAR FIELD IN AN EXPANDING SPACE-TIME

Since the interaction rate for scattering processes between the scalar fermion fields and the thermal bath in the early Universe is found [4] to be of the same order of magnitude as their decay rate Γ_Φ^{-1} (see Sec. II), the scalar fermions are essentially decoupled from the bath for a time scale much longer than the oscillation period of the scalar fields: $m_\Phi^{-1} \ll t \ll \Gamma_\Phi^{-1}$. We can therefore apply the method of nonequilibrium quantum field theory with zero temperature to study Affleck-Dine baryogenesis by considering the model of Eq. (2).

The relevant action can be written as

$$S = \int d^4x \sqrt{-g} [g_{\mu\nu} (\partial^\mu \Phi^\dagger)(\partial^\nu \Phi) - m_\Phi^2 \Phi^\dagger \Phi - i\lambda(\Phi^4 - \Phi^{\dagger 4})]. \tag{20}$$

The background geometry is governed by the spatially flat Robertson-Walker metric,

$$d^2 s = d^2 t - a^2(t) d^2 \mathbf{x}, \tag{21}$$

where $a(t)$ is a scale factor. It will be convenient to introduce the conformal time η defined as $d\eta = a^{-1} dt$ and the conformally rescaled field, $\chi = a\Phi$, whereby the above action can be written as that of a complex scalar field in flat space-time with a time-dependent mass term. To see this, we express the complex scalar field χ in terms of its real and imaginary parts: $\chi = (1/\sqrt{2})(\chi_1 + i\chi_2)$.

The action becomes

$$S = \int d\eta d^3\mathbf{x}\,\mathcal{L}[\chi_1, \chi_2] = \int d\eta d^3\mathbf{x}\Big[\frac{1}{2}\chi_1'^2 - \frac{1}{2}(\vec{\nabla}\chi_1)^2 + \frac{1}{2}\chi_2'^2 - \frac{1}{2}(\vec{\nabla}\chi_2)^2 - U(\chi_1, \chi_2)\Big], \tag{22}$$

where $\chi_i' \equiv \partial\chi_i/\partial\eta$ and the new potential

$$U(\chi_1, \chi_2) = \frac{1}{2}m_\chi^2(\eta)(\chi_1^2 + \chi_2^2) - 2\lambda\chi_1\chi_2(\chi_1^2 - \chi_2^2) \tag{23}$$

has the time-dependent mass term with $m_\chi^2(\eta) = m_\Phi^2 a^2 - (a''/a)$.

Since we are interested in the effects of the quantum fluctuations of the scalar fields χ_1 and χ_2, it will be useful to express each of them in terms of its expectation value with respect to an initial density matrix that will be specified later and the fluctuation field around this average value:

$$\chi_1^\pm(\mathbf{x}, \eta) = \chi_1^0(\eta) + \tilde{\chi}_1^\pm(\mathbf{x}, \eta), \qquad \langle\chi_1^\pm(\mathbf{x}, \eta)\rangle = \chi_1^0(\eta);$$
$$\chi_2^\pm(\mathbf{x}, \eta) = \chi_2^0(\eta) + \tilde{\chi}_2^\pm(\mathbf{x}, \eta), \qquad \langle\chi_2^\pm(\mathbf{x}, \eta)\rangle = \chi_2^0(\eta). \tag{24}$$

We have listed the fields belonging to the forward (+) and backward (−) time branches explicitly. The reason for shifting the (±) fields by the same configuration is that the field expectation values enter in the time evolution operator as c-number background fields, and the evolution forward and backward are considered in this background [9]. Note that χ_1^0 and χ_2^0 are time-dependent for the nonequilibrium problem. We will implement later the corresponding tadpole conditions, $\langle\tilde{\chi}_1^\pm(\mathbf{x}, \eta)\rangle = 0$ and $\langle\tilde{\chi}_2^\pm(\mathbf{x}, \eta)\rangle = 0$, to derive the equations of motion for these field expectation values. Expanding the action in terms of the fluctuation fields $\tilde{\chi}_1(\mathbf{x}, \eta)$ and $\tilde{\chi}_2(\mathbf{x}, \eta)$, the Lagrangian density becomes

$$\begin{aligned}\mathcal{L}[\chi_1^0 + \tilde{\chi}_1^+, \chi_2^0 + \tilde{\chi}_2^+] = {} & \mathcal{L}[\chi_1^0, \chi_2^0] + \mathcal{L}[\tilde{\chi}_1^+, \tilde{\chi}_2^+] - \tilde{\chi}_1^+\{\chi_1^{0\prime\prime} + m_\chi^2(\eta)\chi_1^0 - 2\lambda[3(\chi_1^0)^2\chi_2^0 - (\chi_2^0)^3]\} \\ & - \tilde{\chi}_2^+\{\chi_2^{0\prime\prime} + m_\chi^2(\eta)\chi_2^0 + 2\lambda[3\chi_1^0(\chi_2^0)^2 - (\chi_1^0)^3]\} + 6\lambda\chi_1^0\chi_2^0(\tilde{\chi}_1^{+2} - \tilde{\chi}_2^{+2}) \\ & + 6\lambda\tilde{\chi}_1^+\tilde{\chi}_2^+[(\chi_1^0)^2 - (\chi_2^0)^2] + 2\lambda(\chi_2^0\tilde{\chi}_1^{+3} - \chi_1^0\tilde{\chi}_2^{+3} + 3\chi_1^0\tilde{\chi}_1^{+2}\tilde{\chi}_2^+ - 3\chi_2^0\tilde{\chi}_1^+\tilde{\chi}_2^{+2})\end{aligned} \tag{25}$$

and similarly for $\mathcal{L}[\chi_1^0 + \tilde{\chi}_1^-, \chi_2^0 + \tilde{\chi}_2^-]$.

We now introduce a Hartree factorization to take account of the quantum fluctuations. The Hartree factorization can be employed for both the (+) and (−) fields as follows:

$$\begin{aligned}\tilde{\chi}_1^3 &\approx 3\langle\tilde{\chi}_1^2\rangle\tilde{\chi}_1, \\ \tilde{\chi}_2^3 &\approx 3\langle\tilde{\chi}_2^2\rangle\tilde{\chi}_2, \\ \tilde{\chi}_1^2\tilde{\chi}_2 &\approx 2\langle\tilde{\chi}_1\tilde{\chi}_2\rangle\tilde{\chi}_1 + \langle\tilde{\chi}_1^2\rangle\tilde{\chi}_2, \\ \tilde{\chi}_1\tilde{\chi}_2^2 &\approx 2\langle\tilde{\chi}_1\tilde{\chi}_2\rangle\tilde{\chi}_2 + \langle\tilde{\chi}_2^2\rangle\tilde{\chi}_1, \\ \tilde{\chi}_1^3\tilde{\chi}_2 &\approx 3\langle\tilde{\chi}_1\tilde{\chi}_2\rangle\tilde{\chi}_1^2 + 3\langle\tilde{\chi}_1^2\rangle\tilde{\chi}_1\tilde{\chi}_2, \\ \tilde{\chi}_1\tilde{\chi}_2^3 &\approx 3\langle\tilde{\chi}_1\tilde{\chi}_2\rangle\tilde{\chi}_2^2 + 3\langle\tilde{\chi}_2^2\rangle\tilde{\chi}_1\tilde{\chi}_2,\end{aligned} \tag{26}$$

where the one-loop corrections to the 2-point Green functions of $\tilde{\chi}_1$ and $\tilde{\chi}_2$ are cancelled by the counterterms introduced above. We would like to point out that the Hartree approximation we adopt here is uncontrolled in the model of Eq. (2). It will be controlled, for example, in alternative models in which the scalar fields are in the vector representation of the symmetry group $O(N)$ as the Hartree approximation is then equivalent to the large-N approximation. Our justification for using this approximation here is simply based on the virtue that it provides a nonperturbative framework to treat the quantum fluctuations by solving the evolution equations self-consistently.

After applying the above factorizations, the nonequilibrium Lagrangian density can be written as

$$\mathcal{L}[\chi_1^0 + \tilde{\chi}_1^+, \chi_2^0 + \tilde{\chi}_2^+] - \mathcal{L}[\chi_1^0 + \tilde{\chi}_1^-, \chi_2^0 + \tilde{\chi}_2^-] = \mathcal{L}_0[\tilde{\chi}_1^+, \tilde{\chi}_2^+] - \mathcal{L}_0[\tilde{\chi}_1^-, \tilde{\chi}_2^-] + \mathcal{L}_{\rm int}[\tilde{\chi}_1^+, \tilde{\chi}_2^+] - \mathcal{L}_{\rm int}[\tilde{\chi}_1^-, \tilde{\chi}_2^-], \tag{27}$$

where

$$\mathcal{L}_0[\tilde{\chi}_1^+, \tilde{\chi}_2^+] = \frac{1}{2}\tilde{\chi}_1^{+\prime 2} - \frac{1}{2}(\vec{\nabla}\tilde{\chi}_1^+)^2 - \frac{1}{2}\mathcal{M}_{\chi_1}^2(\eta)\tilde{\chi}_1^{+2} + \frac{1}{2}\tilde{\chi}_2^{+\prime 2} - \frac{1}{2}(\vec{\nabla}\tilde{\chi}_2^+)^2 - \frac{1}{2}\mathcal{M}_{\chi_2}^2(\eta)\tilde{\chi}_2^{+2}, \tag{28}$$

with

$$\mathcal{M}_{\chi_1}^2(\eta) = m_\chi^2(\eta) - 12\lambda\chi_1^0\chi_2^0 - 12\lambda\langle\tilde{\chi}_1\tilde{\chi}_2\rangle, \qquad \mathcal{M}_{\chi_2}^2(\eta) = m_\chi^2(\eta) + 12\lambda\chi_1^0\chi_2^0 + 12\lambda\langle\tilde{\chi}_1\tilde{\chi}_2\rangle, \tag{29}$$

and

$$\mathcal{L}_{\rm int}[\tilde{\chi}_1^+, \tilde{\chi}_2^+] = -\alpha_1(\eta)\tilde{\chi}_1^+ - \alpha_2(\eta)\tilde{\chi}_2^+ + \alpha_{12}(\eta)\tilde{\chi}_1^+\tilde{\chi}_2^+, \tag{30}$$

with the couplings

$$\begin{aligned}\alpha_1(\eta) &= \chi_1^{0''} + m_\chi^2(\eta)\chi_1^0 - 2\lambda[3(\chi_1^0)^2\chi_2^0 - (\chi_2^0)^3] \\ &\quad - 6\lambda\chi_2^0(\langle\tilde{\chi}_1^2\rangle - \langle\tilde{\chi}_2^2\rangle) - 12\lambda\chi_1^0\langle\tilde{\chi}_1\tilde{\chi}_2\rangle, \\ \alpha_2(\eta) &= \chi_2^{0''} + m_\chi^2(\eta)\chi_2^0 + 2\lambda[3\chi_1^0(\chi_2^0)^2 - (\chi_1^0)^3] \\ &\quad - 6\lambda\chi_1^0(\langle\tilde{\chi}_1^2\rangle - \langle\tilde{\chi}_2^2\rangle) + 12\lambda\chi_2^0\langle\tilde{\chi}_1\tilde{\chi}_2\rangle, \\ \alpha_{12}(\eta) &= 6\lambda[(\chi_1^0)^2 - (\chi_2^0)^2] + 6\lambda(\langle\tilde{\chi}_1^2\rangle - \langle\tilde{\chi}_2^2\rangle).\end{aligned} \tag{31}$$

We have used the fact that correlation functions of fields evaluated at the same space-time point in the forward and backward time branches are equal. This can be seen from Eq. (18) by identifying $(\mathbf{x}, t)$ with $(\mathbf{x}', t')$. In addition, due to the spatial translational invariance, the correlation functions depend only on time and should be understood as: $\langle\tilde{\chi}_1^+(\mathbf{x}, \eta)\tilde{\chi}_2^+(\mathbf{x}, \eta)\rangle = \langle\tilde{\chi}_1^-(\mathbf{x}, \eta)\tilde{\chi}_2^-(\mathbf{x}, \eta)\rangle = \langle\tilde{\chi}_1\tilde{\chi}_2\rangle(\eta)$, $\langle\tilde{\chi}_i^{+2}(\mathbf{x}, \eta)\rangle = \langle\tilde{\chi}_i^{-2}(\mathbf{x}, \eta)\rangle = \langle\tilde{\chi}_i^2\rangle(\eta) (i = 1, 2)$.

In Eq. (27), $\mathcal{L}_0$ is the unperturbed quadratic Lagrangian with respect to which the nonequilibrium Green functions will be defined and the interaction Lagrangian $\mathcal{L}_{\rm int}$ contains the linear terms in $\tilde{\chi}_i$ as well as the $\tilde{\chi}_1\tilde{\chi}_2$ terms which will be treated as perturbations. The presence of the nondiagonal $\tilde{\chi}_1\tilde{\chi}_2$ terms implies that these fields do not form a good basis to construct the nonequilibrium propagators in a perturbative expansion. One may therefore consider invoking the Bogoliubov transformation which is a canonical transformation in the sense that it leaves the measure of the path-integral invariant. In this case, the transformation is a two-dimensional field rotation between the old and new basis fields with one parameter specified by the rotation angle. The angle for the field rotation can be determined so as to rid the nondiagonal term in the potential energy of the Lagrangian. In the presence of the time-dependent background fields, it turns out that the Bogoliubov transformation acquires a time-dependent rotation angle, which in turn gives rise to a new kind of unwanted nondiagonal terms in the kinetic energy. Thus, it seems that the Bogoliubov transformation fails to diagonalize the Lagrangian in the presence of the time-dependent background fields. To proceed, we can further approximate the term $\tilde{\chi}_1\tilde{\chi}_2$ by its mean value $\langle\tilde{\chi}_1\tilde{\chi}_2\rangle$. In other words, we write

$$\tilde{\chi}_1\tilde{\chi}_2 = \langle\tilde{\chi}_1\tilde{\chi}_2\rangle + (\tilde{\chi}_1\tilde{\chi}_2 - \langle\tilde{\chi}_1\tilde{\chi}_2\rangle), \tag{32}$$

and treat the terms in the parenthesis as a perturbation.

The fluctuation fields can be decomposed in terms of their Fourier modes with time-dependent mode functions as

$$\begin{aligned}\tilde{\chi}_i(\mathbf{x}, \eta) &= \frac{1}{\sqrt{\Omega}}\sum_{\mathbf{k}}\tilde{\chi}_{i,\mathbf{k}}(\eta)e^{i\mathbf{k}\cdot\mathbf{x}} \\ &= \frac{1}{\sqrt{\Omega}}\sum_{\mathbf{k}}[a_{i,\mathbf{k}}f_{i,\mathbf{k}}(\eta) + a_{i,-\mathbf{k}}^\dagger f_{i,-\mathbf{k}}^*(\eta)]e^{i\mathbf{k}\cdot\mathbf{x}}, \\ i &= 1, 2,\end{aligned} \tag{33}$$

where $a_{i,\mathbf{k}}$ and $a_{i,-\mathbf{k}}^\dagger$ are, respectively, the annihilation and creation operators for the fluctuation field $\tilde{\chi}_i$ with momentum $\mathbf{k}$. The equations of motion for the mode functions $f_{i,\mathbf{k}}$ can be read off from the quadratic Lagrangian $\mathcal{L}_0$ in Eq. (28) as

$$\left[\frac{d^2}{d\eta^2} + k^2 + \mathcal{M}_{\chi_i}^2(\eta)\right]f_{i,\mathbf{k}}(\eta) = 0, \qquad i = 1, 2 \tag{34}$$

where $k^2 = \mathbf{k}\cdot\mathbf{k}$. The nonequilibrium propagators can also be expressed in terms of the mode functions:

$$\begin{aligned}G_{i,\mathbf{k}}^{++}(\eta, \eta') &= G_{i,\mathbf{k}}^{>}(\eta, \eta')\Theta(\eta - \eta') \\ &\quad + G_{i,\mathbf{k}}^{<}(\eta, \eta')\Theta(\eta' - \eta), \\ G_{i,\mathbf{k}}^{--}(\eta, \eta') &= G_{i,\mathbf{k}}^{>}(\eta, \eta')\Theta(\eta' - \eta) \\ &\quad + G_{i,\mathbf{k}}^{<}(\eta, \eta')\Theta(\eta - \eta'), \\ G_{i,\mathbf{k}}^{+-}(\eta, \eta') &= G_{i,\mathbf{k}}^{<}(\eta, \eta'), \\ G_{i,\mathbf{k}}^{-+}(\eta, \eta') &= G_{i,\mathbf{k}}^{>}(\eta, \eta'), \\ G_{i,\mathbf{k}}^{>}(\eta, \eta') &= \int d^3\mathbf{x}\langle\tilde{\chi}_i(\mathbf{x}, \eta)\tilde{\chi}_i(\mathbf{0}, \eta')\rangle e^{-i\mathbf{k}\cdot\mathbf{x}} \\ &= f_{i,\mathbf{k}}(\eta)f_{i,\mathbf{k}}^*(\eta'), \\ G_{i,\mathbf{k}}^{<}(\eta, \eta') &= \int d^3\mathbf{x}\langle\tilde{\chi}_i(\mathbf{0}, \eta')\tilde{\chi}_i(\mathbf{x}, \eta)\rangle e^{-i\mathbf{k}\cdot\mathbf{x}} \\ &= f_{i,\mathbf{k}}(\eta')f_{i,\mathbf{k}}^*(\eta),\end{aligned} \tag{35}$$

where the correlations of the fluctuation fields are taken with respect to a vacuum state that is annihilated by the $a_{i,\mathbf{k}}$ of Eq. (33).

The equations of motion for the expectation values of the fields can be obtained from the tadpole conditions. From the condition $\langle\tilde{\chi}_1^+(\mathbf{x}, \eta)\rangle = 0$, the lowest-order contributions to the equation of motion are obtained from the terms linear in $\tilde{\chi}_1^+$ in the interaction Lagrangian (30). We find

$$\int d\eta[-\alpha_1(\eta)\langle\tilde{\chi}_1^+\tilde{\chi}_1^+\rangle + \alpha_1(\eta)\langle\tilde{\chi}_1^+\tilde{\chi}_1^-\rangle] = 0, \tag{36}$$

where the spatial arguments have been suppressed. Since the correlation functions $\langle\tilde{\chi}_1^+\tilde{\chi}_1^+\rangle$ and $\langle\tilde{\chi}_1^+\tilde{\chi}_1^-\rangle$ are linearly independent, the above equation leads to the equation of motion for χ_1^0:

$$\begin{aligned}\chi_1^{0''} + m_\chi^2(\eta)\chi_1^0 - 2\lambda[3(\chi_1^0)^2\chi_2^0 - (\chi_2^0)^3] - 6\lambda\chi_2^0(\langle\tilde{\chi}_1^2\rangle \\ - \langle\tilde{\chi}_2^2\rangle) - 12\lambda\chi_1^0\langle\tilde{\chi}_1\tilde{\chi}_2\rangle = 0,\end{aligned} \tag{37}$$

where Eq. (31) has been used. It is straightforward to see that implementing the condition $\langle\tilde{\chi}_1^-(\mathbf{x}, \eta)\rangle = 0$ will lead to the same equation of motion for χ_1^0. Following the similar procedure with the conditions $\langle\tilde{\chi}_2^\pm(\mathbf{x}, \eta)\rangle = 0$, we find the equation of motion for χ_2^0 to be

$$\begin{aligned}\chi_2^{0''} + m_\chi^2(\eta)\chi_2^0 + 2\lambda[3\chi_1^0(\chi_2^0)^2 - (\chi_1^0)^3] - 6\lambda\chi_1^0(\langle\tilde{\chi}_1^2\rangle \\ - \langle\tilde{\chi}_2^2\rangle) + 12\lambda\chi_2^0\langle\tilde{\chi}_1\tilde{\chi}_2\rangle = 0.\end{aligned} \tag{38}$$

The quantum fluctuations $\langle\tilde{\chi}_1^2\rangle$ and $\langle\tilde{\chi}_2^2\rangle$ can be determined self-consistently and have the form

$$\langle\tilde{\chi}_i^2\rangle(\eta) = \int \frac{d^3\mathbf{k}}{(2\pi)^3} \mid f_{i,\mathbf{k}}(\eta) \mid^2, \tag{39}$$

where the infinite volume limit has been taken. On the other hand, the term $\langle\tilde{\chi}_1\tilde{\chi}_2\rangle$ vanishes at tree level and one has to include an interaction vertex from the perturbations to obtain its loop corrections. To lowest order in perturbation theory, the vertex $6i\lambda[(\chi_1^0)^2 - (\chi_2^0)^2]\tilde{\chi}_1\tilde{\chi}_2$ is included and one finds that

$$\begin{aligned}
\langle\tilde{\chi}_1\tilde{\chi}_2\rangle(\eta) &= \int \frac{d^3\mathbf{k}}{(2\pi)^3}\langle\tilde{\chi}_{1,\mathbf{k}}(\eta)\tilde{\chi}_{2,-\mathbf{k}}(\eta)\rangle \\
&= 6i\lambda\int_{\eta_0}^{\eta} d\eta'\{[\chi_1^0(\eta')]^2 - [\chi_2^0(\eta')]^2\}[\langle\tilde{\chi}_{1,\mathbf{k}}^+(\eta)\tilde{\chi}_{1,-\mathbf{k}}^+(\eta')\rangle\langle\tilde{\chi}_{2,-\mathbf{k}}^+(\eta)\tilde{\chi}_{2,\mathbf{k}}^+(\eta')\rangle - \langle\tilde{\chi}_{1,\mathbf{k}}^+(\eta)\tilde{\chi}_{1,-\mathbf{k}}^-(\eta')\rangle \\
&\quad\times\langle\tilde{\chi}_{2,-\mathbf{k}}^+(\eta)\tilde{\chi}_{2,\mathbf{k}}^-(\eta')\rangle] \\
&= 6i\lambda\int_{\eta_0}^{\eta} d\eta'\{[\chi_1^0(\eta')]^2 - [\chi_2^0(\eta')]^2\}[G_{1,\mathbf{k}}^{>}(\eta,\eta')G_{2,\mathbf{k}}^{>}(\eta,\eta') - G_{1,\mathbf{k}}^{<}(\eta,\eta')G_{2,\mathbf{k}}^{<}(\eta,\eta')]\Theta(\eta-\eta').
\end{aligned} \tag{40}$$

As mentioned earlier, the η_0 dependence arises from the perturbations being switched on at time η_0. We have shown above only the calculation (second equality) for the $\tilde{\chi}_1^+\tilde{\chi}_2^+$ correlation. However, as we have stated after Eq. (31), the final result is also applicable to $\langle\tilde{\chi}_1^-\tilde{\chi}_2^-\rangle$. In terms of the mode functions, this correlation function becomes

$$\langle\tilde{\chi}_1\tilde{\chi}_2\rangle(\eta) = 6i\lambda\int_{\eta_0}^{\eta} d\eta'\{[\chi_1^0(\eta')]^2 - [\chi_2^0(\eta')]^2\}[f_{1,\mathbf{k}}(\eta)f_{1,\mathbf{k}}^*(\eta')f_{2,\mathbf{k}}(\eta)f_{2,\mathbf{k}}^*(\eta') - \text{c.c.}]. \tag{41}$$

Eqs. (34), (37)–(39), and (41) form the full set of coupled equations from which we will solve for the field expectation values and the mode functions.

V. NONEQUILIBRIUM EFFECTS AND BARYON ASYMMETRY

The proper normalization to measure baryon asymmetry is given by the particle number density. Let us consider the initial state at time t_0 to be specified by the adiabatic modes for uncoupled harmonic oscillations defined in cosmic time under Hartree approximations. The corresponding initial particle number density can be expressed as

$$\begin{aligned}
\hat{n}(t_0) = \int \frac{d^3\mathbf{k}}{(2\pi)^3}\Big\{&\frac{a^3(t_0)}{2\mathcal{W}_{1,\mathbf{k}}(t_0)}[\dot{\Phi}_{1,\mathbf{k}}(t_0)\dot{\Phi}_{1,-\mathbf{k}}(t_0) + \mathcal{W}_{1,\mathbf{k}}^2(t_0)\Phi_{1,\mathbf{k}}(t_0)\Phi_{1,-\mathbf{k}}(t_0)] \\
&+ \frac{a^3(t_0)}{2\mathcal{W}_{2,\mathbf{k}}(t_0)}[\dot{\Phi}_{2,\mathbf{k}}(t_0)\dot{\Phi}_{2,-\mathbf{k}}(t_0) + \mathcal{W}_{2,\mathbf{k}}^2(t_0)\Phi_{2,\mathbf{k}}(t_0)\Phi_{2,-\mathbf{k}}(t_0)] - 1\Big\},
\end{aligned} \tag{42}$$

where $\Phi = (\Phi_1 + i\Phi_2)/\sqrt{2}$. The instantaneous frequencies for the real and imaginary part of the complex scalar field Φ can be gleaned from Eqs. (34) and (29) to be

$$\begin{aligned}
\mathcal{W}_{1,\mathbf{k}}(t_0) &= \left[\frac{k^2}{a^2(t_0)} + m_\Phi^2 - 12\lambda a^{-2}(t_0)(\chi_1^0(t_0)\chi_2^0(t_0) + \langle\tilde{\chi}_1\tilde{\chi}_2\rangle(t_0))\right]^{1/2}, \\
\mathcal{W}_{2,\mathbf{k}}(t_0) &= \left[\frac{k^2}{a^2(t_0)} + m_\Phi^2 + 12\lambda a^{-2}(t_0)(\chi_1^0(t_0)\chi_2^0(t_0) + \langle\tilde{\chi}_1\tilde{\chi}_2\rangle(t_0))\right]^{1/2}.
\end{aligned} \tag{43}$$

The expectation value of the number operator with respect to an initial vacuum state as defined after Eq. (35) evolves in time and has the following form in the Heisenberg picture:

$$\begin{aligned}
\langle\hat{n}\rangle(t) = \int \frac{d^3\mathbf{k}}{(2\pi)^3}\Big\{&\frac{a^3(t_0)}{2\mathcal{W}_{1,\mathbf{k}}(t_0)}[\langle\dot{\Phi}_{1,\mathbf{k}}(t)\dot{\Phi}_{1,-\mathbf{k}}(t)\rangle + \mathcal{W}_{1,\mathbf{k}}^2(t_0)\langle\Phi_{1,\mathbf{k}}(t)\Phi_{1,-\mathbf{k}}(t)\rangle] \\
&+ \frac{a^3(t_0)}{2\mathcal{W}_{2,\mathbf{k}}(t_0)}[\langle\dot{\Phi}_{2,\mathbf{k}}(t)\dot{\Phi}_{2,-\mathbf{k}}(t)\rangle + \mathcal{W}_{2,\mathbf{k}}^2(t_0)\langle\Phi_{2,\mathbf{k}}(t)\Phi_{2,-\mathbf{k}}(t)\rangle] - 1\Big\}.
\end{aligned} \tag{44}$$

In terms of the conformally rescaled fields, the expectation value of the particle number density can be written as the mean

value constructed from the expectation values of the quantum fields plus its quantum fluctuations:

$$\begin{aligned}
&\langle\hat{n}\rangle(\eta) \equiv n(\eta) = n_0(\eta) + n_{\rm q}(\eta),\\
&n_0(\eta) = \frac{a^3(\eta_0)}{2\mathcal{W}_{1,\mathbf{0}}(\eta_0)a^4(\eta)}\left\{\left[\frac{d}{d\eta}\chi_1^0(\eta)\right]^2 - \frac{a'(\eta)}{a(\eta)}\frac{d}{d\eta}[\chi_1^0(\eta)]^2 + \Omega_{1,\mathbf{k}}(\eta)[\chi_1^0(\eta)]^2\right\} + (\chi_1 \to \chi_2; \Omega_{1,\mathbf{k}}(\eta) \to \Omega_{2,\mathbf{k}}(\eta)),\\
&n_{\rm q}(\eta) = \int\frac{d^3\mathbf{k}}{(2\pi)^3}\left\{\frac{a^3(\eta_0)}{2\mathcal{W}_{1,\mathbf{k}}(\eta_0)a^4(\eta)}[\langle\tilde{\chi}'_{1,\mathbf{k}}(\eta)\tilde{\chi}'_{1,-\mathbf{k}}(\eta)\rangle - \frac{a'(\eta)}{a(\eta)}\left(\frac{d}{d\eta}\langle\tilde{\chi}_{1,\mathbf{k}}(\eta)\tilde{\chi}_{1,-\mathbf{k}}(\eta)\rangle\right)\right.\\
&\qquad\left. + \Omega_{1,\mathbf{k}}(\eta)\langle\tilde{\chi}_{1,\mathbf{k}}(\eta)\tilde{\chi}_{1,-\mathbf{k}}(\eta)\rangle\right] - \frac{1}{2}\right\} + (\tilde{\chi}_1 \to \tilde{\chi}_2; \Omega_{1,\mathbf{k}}(\eta) \to \Omega_{2,\mathbf{k}}(\eta)),
\end{aligned} \tag{45}$$

where

$$\Omega_{i,\mathbf{k}}(\eta) = \mathcal{W}^2_{i,\mathbf{k}}(\eta_0)a^2(\eta) + \frac{a'^2(\eta)}{a^2(\eta)} \tag{46}$$

and $\eta_0 \equiv \eta(t_0)$ is the initial conformal time.

The correlation functions can be expressed in terms of the mode functions as in Eq. (39):

$$\begin{aligned}
\langle\tilde{\chi}'_{i,\mathbf{k}}(\eta)\tilde{\chi}'_{i,-\mathbf{k}}(\eta)\rangle &= |f'_{i,\mathbf{k}}(\eta)|^2,\\
\langle\tilde{\chi}_{i,\mathbf{k}}(\eta)\tilde{\chi}_{i,-\mathbf{k}}(\eta)\rangle &= |f_{i,\mathbf{k}}(\eta)|^2.
\end{aligned} \tag{47}$$

In the weak coupling limit, and with appropriate choices for the initial expectation values of the quantum fields, we may approximate

$$\begin{aligned}
&\mathcal{W}_{1,\mathbf{k}}(t_0) \approx \mathcal{W}_{2,\mathbf{k}}(t_0) \approx \mathcal{W}_{\mathbf{k}}(t_0);\\
&\mathcal{W}_{\mathbf{k}}(t_0) = \left[\frac{k^2}{a^2(t_0)} + m^2_\Phi\right]^{1/2}.
\end{aligned} \tag{48}$$

This approximation simplifies the expression for the baryon-number density which is given by the current in Eq. (3): $\hat{n}_{\rm B} = i(\Phi^\dagger\dot{\Phi} - \dot{\Phi}^\dagger\Phi)$. In parallel with the discussion above for the particle number density, we find

$$\begin{aligned}
\hat{n}_{\rm B}(t) = \frac{a^3(t_0)}{2}\int\frac{d^3\mathbf{k}}{(2\pi)^3} i[&\Phi^\dagger_{-\mathbf{k}}(t)\dot{\Phi}_{\mathbf{k}}(t) + \dot{\Phi}_{-\mathbf{k}}(t)\Phi^\dagger_{\mathbf{k}}(t)\\
&- \dot{\Phi}^\dagger_{-\mathbf{k}}(t)\Phi_{\mathbf{k}}(t) - \Phi_{-\mathbf{k}}(t)\dot{\Phi}^\dagger_{\mathbf{k}}(t)].
\end{aligned} \tag{49}$$

After converting to conformal time, the expectation value of the baryon-number density is found to be

$$\begin{aligned}
n_{\rm B}(\eta) &\equiv \langle\hat{n}_{\rm B}\rangle(\eta)\\
&= \frac{a^3(\eta_0)}{a^3(\eta)}(\chi_2^0(\eta)\chi_1^{0'}(\eta) - \chi_1^0(\eta)\chi_2^{0'}(\eta))\\
&\quad + \frac{a^3(\eta_0)}{a^3(\eta)}\int\frac{d^3\mathbf{k}}{(2\pi)^3}[\langle\tilde{\chi}'_{1,\mathbf{k}}(\eta)\tilde{\chi}_{2,-\mathbf{k}}(\eta)\rangle\\
&\quad - \langle\tilde{\chi}_{1,\mathbf{k}}(\eta)\tilde{\chi}'_{2,-\mathbf{k}}(\eta)\rangle].
\end{aligned} \tag{50}$$

Like the particle number density, it can be separated into a mean value plus its quantum fluctuations. Just as in the earlier computation for the term $\langle\tilde{\chi}_1\tilde{\chi}_2\rangle$, the quantum fluctuations can be computed by introducing a vertex $6i\lambda[(\chi_1^0)^2 - (\chi_2^0)^2]\tilde{\chi}_1\tilde{\chi}_2$ at the lowest order, which yields

$$\begin{aligned}
n_{\rm B}(\eta) &= \frac{a^3(\eta_0)}{a^3(\eta)}(\chi_2^0(\eta)\chi_1^{0'}(\eta) - \chi_1^0(\eta)\chi_2^{0'}(\eta))\\
&\quad + 6ia^3(\eta_0)\lambda\int_{\eta_0}^{\eta} d\eta'\{[\chi_1^0(\eta')]^2 - [\chi_2^0(\eta')]^2\}\\
&\quad \times\{[f'_{1,\mathbf{k}}(\eta)f^*_{1,\mathbf{k}}(\eta')f_{2,\mathbf{k}}(\eta)f^*_{2,\mathbf{k}}(\eta') - \text{c.c.}]\\
&\quad - [f_{1,\mathbf{k}}(\eta)f^*_{1,\mathbf{k}}(\eta')f'_{2,\mathbf{k}}(\eta)f^*_{2,\mathbf{k}}(\eta') - \text{c.c.}]\}.
\end{aligned} \tag{51}$$

The baryon-number density can be evaluated once the mode functions and field expectation values are determined by the method described in Sec. IV. In order to ensure the canonical quantization rules, the mode functions must satisfy the relation

$$f'_{i,\mathbf{k}}(\eta)f^*_{i,\mathbf{k}}(\eta) - f_{i,\mathbf{k}}(\eta)f^{*\prime}_{i,\mathbf{k}}(\eta) = -i, \tag{52}$$

which follows from the mode Eqs. (34). With the initial states described by the adiabatic modes for uncoupled harmonic oscillations, the mode functions have the following initial values at the conformal time η_0:

$$\begin{aligned}
f_{i,\mathbf{k}}(\eta_0) &= \frac{a(\eta_0)}{\sqrt{2a^3(\eta_0)\mathcal{W}_{\mathbf{k}}(\eta_0)}},\\
f'_{i,\mathbf{k}}(\eta_0) &= \frac{a'(\eta_0)}{\sqrt{2a^3(\eta_0)\mathcal{W}_{\mathbf{k}}(\eta_0)}} - i\frac{a^2(\eta_0)\mathcal{W}_{\mathbf{k}}(\eta_0)}{\sqrt{2a^3(\eta_0)\mathcal{W}_{\mathbf{k}}(\eta_0)}}.
\end{aligned} \tag{53}$$

As expected, these initial conditions guarantee that the baryon and particle number densities have zero quantum fluctuations initially.

Consistent with the initial conditions (5), the initial expectation values of the conformally rescaled fields are

$$\begin{aligned}
\chi_1^0(\eta_0) = 0, \qquad \chi_1^{0'}(\eta_0) = 0;\\
\chi_2^0(\eta_0) = \sqrt{2}a(\eta_0)\Phi_0, \qquad \chi_2^{0'}(\eta_0) = \sqrt{2}a'(\eta_0)\Phi_0.
\end{aligned} \tag{54}$$

Together with (53), these initial conditions guarantee that the initial baryon asymmetry is zero: $n_{\rm B}(\eta_0) = 0$.

In the next section, we will present the results of our calculation that assumes a radiation-dominated epoch in which the scale factor follows $a(\eta) = m_\Phi \eta$. We find that the results are similar in a matter-dominated universe and will not present explicit results for this case.

VI. RESULTS

Before we describe the numerical solutions to the coupled equations, let us try to understand the issue of ultraviolet divergence associated with the loop integrals in these equations. The large-k behavior of the mode functions can be obtained from WKB type solutions to the mode equations:

$$f_{i,\mathbf{k}}(\eta) = \frac{a(\eta_0)}{2\sqrt{2a^3(\eta_0)\mathcal{W}_\mathbf{k}(\eta_0)}} \times [(1+\gamma)\mathcal{D}^*_{i,\mathbf{k}}(\eta) + (1-\gamma)\mathcal{D}_{i,\mathbf{k}}(\eta)], \quad (55)$$

where

$$\mathcal{D}_{i,\mathbf{k}}(\eta) = e^{\int_{\eta_0}^{\eta} \mathcal{R}_{i,\mathbf{k}}(\eta')d\eta'} \quad (56)$$

and

$$\mathcal{R}_{i,\mathbf{k}}(\eta) = -ik - \frac{i}{2k}\mathcal{M}^2_{\chi_i}(\eta) - \frac{1}{4k^2}\frac{d}{d\eta}\mathcal{M}^2_{\chi_i}(\eta) + \mathcal{O}\left(\frac{1}{k^3}\right) + \cdots. \quad (57)$$

The parameter γ that appears in Eq. (55) can be determined from the initial conditions (53) on the mode functions. It has the large-k expansion

$$\gamma = -1 - \frac{i}{k}\left(\frac{a'(\eta_0)}{a(\eta_0)}\right) + \mathcal{O}\left(\frac{1}{k^3}\right) + \cdots, \quad (58)$$

which secures

$$|f_{i,\mathbf{k}}(\eta)|^2 = \frac{1}{2k} - \frac{1}{4k^3}\left(\mathcal{M}^2_{\chi_i}(\eta) - \frac{a'^2(\eta_0)}{a^2(\eta_0)}\right) + \mathcal{O}\left(\frac{1}{k^4}\right) + \cdots. \quad (59)$$

These large-k behaviors lead to quadratic and logarithmic divergence for the loop integrals as follows:

$$\langle\tilde{\chi}^2_i\rangle(\eta) = \frac{\Lambda^2}{8\pi^2} - \frac{1}{8\pi^2}\left(\mathcal{M}^2_{\chi_i}(\eta) - \frac{a'^2(\eta_0)}{a^2(\eta_0)}\right)\ln\frac{\Lambda}{\kappa} + \text{finite}, \quad (60)$$

where Λ is the ultraviolet momentum cutoff and κ is the renormalization scale. Let us recall that the Affleck-Dine model under consideration is used as an effective field theory to describe the relevant low-energy physics from a supersymmetric grand unified theory. Λ is therefore a physical cutoff which can be set at the scale of grand unification, $\Lambda \approx M_G$, while κ can be chosen to be the supersymmetry-breaking scale, $\kappa \approx M_S \approx m_\Phi$. Since the relevant terms involved in the equations for the field expectation values are of the form $(\langle\tilde{\chi}^2_1\rangle - \langle\tilde{\chi}^2_2\rangle)$, only the logarithmic dependence on the cutoff Λ remains. For weak couplings, such a mild cutoff dependence does not present any difficulties for our numerical study. Using Eqs. (55)–(57), the quantum fluctuations $\langle\tilde{\chi}_1\tilde{\chi}_2\rangle$ prove to be ultraviolet safe.

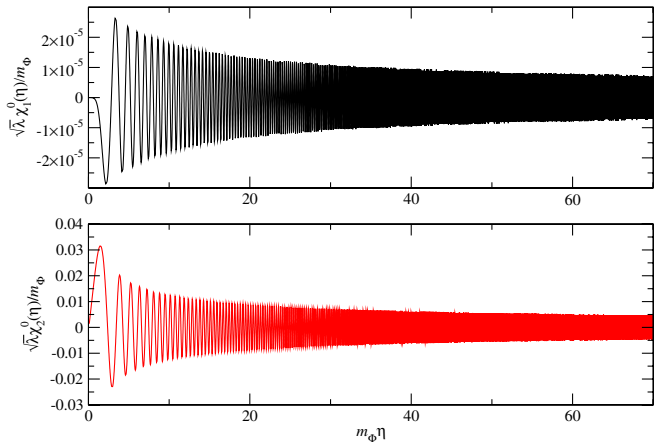

FIG. 1 (color online). Time evolution of the field expectation values χ^0_1 and χ^0_2 for $\phi_0 \equiv \sqrt{\lambda}\Phi_0/m_\Phi = 10^{-2}$ and $\lambda = 10^{-3}$.

Let us turn now to the numerical results of our study. Figure 1 shows the evolution of the expectation values of the quantum fields $\chi^0_1(\eta)$ and $\chi^0_2(\eta)$ in units of $m_\Phi/\sqrt{\lambda}$, the scale of which is set by the dimensionless parameter $\phi_0 \equiv \sqrt{\lambda}\Phi_0/m_\Phi = 10^{-2}$. According to Eqs. (37) and (38), the evolution of the field expectation values are determined by the fluctuations $(\langle\tilde{\chi}^2_1\rangle - \langle\tilde{\chi}^2_2\rangle)(\eta)$ and $\langle\tilde{\chi}_1\tilde{\chi}_2\rangle(\eta)$, which are displayed in Fig. 2.

For an extremely weak coupling, e.g., $\lambda = 10^{-20}$, Fig. 2(a) shows that the quantum fluctuations are very

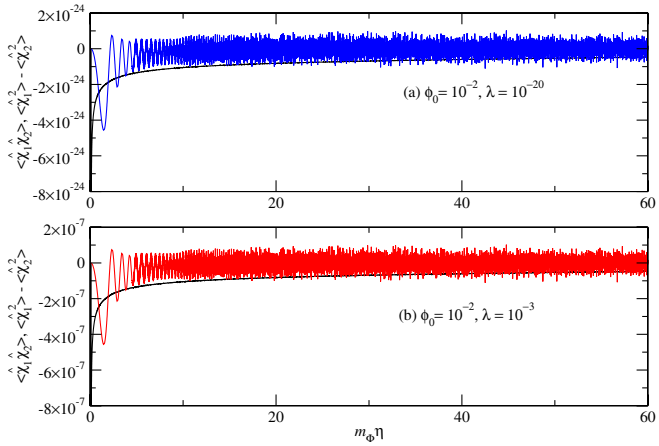

FIG. 2 (color online). Time evolution of $\langle\tilde{\chi}^2_1\rangle - \langle\tilde{\chi}^2_2\rangle$ (smooth curves) and $\langle\tilde{\chi}_1\tilde{\chi}_2\rangle$ (oscillating curves) for $\phi_0 = 10^{-2}$ and (a) $\lambda = 10^{-20}$ and (b) $\lambda = 10^{-3}$. Note that we have used the rescaled fields $\hat{\chi}_i \equiv \sqrt{\lambda}\tilde{\chi}_i/m_\Phi$.

small and $\chi_1^0(\eta)$ and $\chi_2^0(\eta)$ follow essentially their classical trajectories which correspond to oscillations with time-dependent frequencies. For a larger, but still weak, coupling (e.g., $\lambda = 10^{-3}$), the fluctuations become more significant [see Fig. 2(b)] and the amplitudes of the oscillations of χ_1^0 and χ_2^0 become damped, as can be seen from Fig. 1. From Eq. (37) and the initial conditions (54), we can estimate the order of magnitude of $\chi_1^0(\eta)$ to be

$$\chi_1^0(\eta) \approx \lambda \frac{[\chi_2^0(\eta)]^3}{m_\Phi^2}, \tag{61}$$

which is consistent with Fig. 1.

The time evolution of the baryon asymmetry, as measured by the ratio of the baryon-number density to the particle number density, $r(\eta) = n_B(\eta)/n(\eta)$, is shown in Fig. 3. As stated earlier, the initial baryon asymmetry is zero due to the initial conditions in Eqs. (53) and (54). For very weak couplings, the evolution of r is determined by the classical dynamics and is depicted in Fig. 3(a). It starts from zero and decreases toward an equilibrium value $r(\infty) \approx -10\phi_0^2$. This saturation value can be understood as follows:

$$|r(\infty)| = \frac{|n_B(\infty)|}{n(\infty)} \approx \frac{\chi_1^0 \chi_2^0}{(\chi_2^0)^2} \approx \left[\frac{\lambda(\chi_2^0)^4}{m_\Phi^2}\right]\left[\frac{1}{(\chi_2^0)^2}\right] \approx \frac{\lambda \Phi_0^2}{m_\Phi^2}, \tag{62}$$

where the approximation for χ_1^0 in Eq. (61) has been applied to compute the baryon-number density n_B, but neglected in the number density n as compared with that of χ_2^0. The negative baryon asymmetry should not be a concern as the sign can be fixed by the baryon-number assignment for the field Φ. The alert reader will recognize that the estimate of $r(\infty)$ above is nothing but the result quoted in Eq. (6).

As can be seen from Fig. 3(b), an interesting phenomenon occurs for larger couplings when the quantum fluctuations become large, typically of the order of the field expectation values. The growth of quantum fluctuations is a consequence of parametric amplification [12,15] induced by the oscillating mean fields. In this case the part of the ratio $r(\eta)$ generated from the quantum fluctuations turns out to dilute the mean-field contribution, and therefore drives the ratio toward a much smaller equilibrium value: $|r(\infty)| \approx 10^{-5}\lambda\Phi_0^4/m_\Phi^4$. It thus appears that, under appropriate conditions, the effects of the nonequilibrium quantum fluctuations can wash out the baryon asymmetry generated from the classical dynamics. The reason for this may be understood as follows. The set of coupled equations, Eqs. (34), (37)–(39), and (41), which we solve to obtain the baryon asymmetry, involves fluctuation terms with nonzero baryon number such as $(\langle\tilde{\chi}_1^2\rangle - \langle\tilde{\chi}_2^2\rangle)$ and $\langle\tilde{\chi}_1\tilde{\chi}_2\rangle$. As such, the amount of baryon asymmetry that can be generated is limited by the Hartree approximation implemented in these equations. On the other hand, as a result of the nature of the couplings under consideration, it is possible to create a large particle number density from the fluctuation term $(\langle\tilde{\chi}_1^2\rangle + \langle\tilde{\chi}_2^2\rangle)$, which has nonzero particle number but zero baryon number under the global $U(1)$ symmetry. This can be seen in Fig. 4, which shows that for a sufficiently large coupling the total particle number density deviates substantially from its classical value, while the baryon-number density remains close to its classical value. A similar plot for a much weaker coupling, e.g., $\lambda = 10^{-20}$, would show that both the particle number density and the baryon-number density remain essentially at their respective classical values. We are thus led to the conclusion that the ratio r can be reduced significantly through nonequilibrium quantum fluctuations with a proper choice of the couplings.

Figure 5 shows the saturation values of r as a function of the coupling λ for a wide range of values of Φ_0. Plotted are

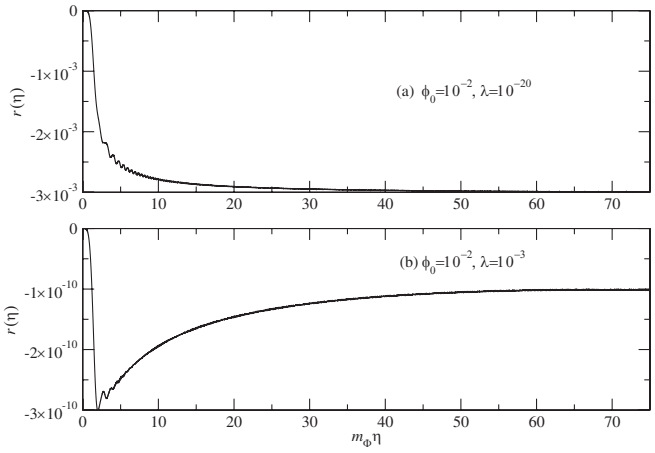

FIG. 3. Time evolution of the ratio of the baryon to particle number density, $r(\eta) = n_B(\eta)/n(\eta)$, for $\phi_0 = 10^{-2}$ and (a) $\lambda = 10^{-20}$ and (b) $\lambda = 10^{-3}$.

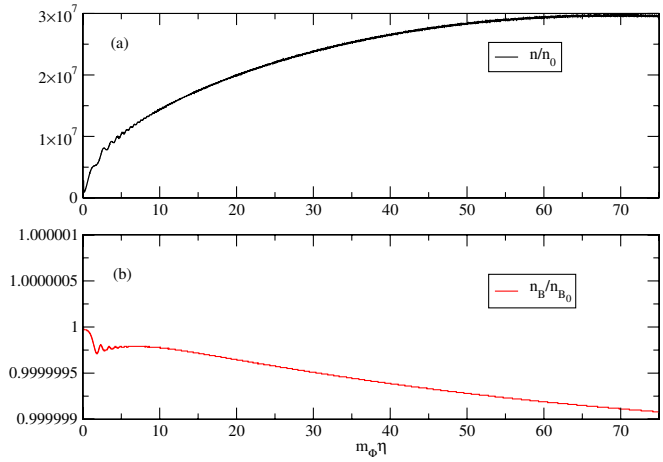

FIG. 4 (color online). (a) Time evolution of the ratio of the total particle number density to its classical value for $\phi_0 = 10^{-2}$ and $\lambda = 10^{-3}$. (b) Same as (a) but for the baryon-number density.

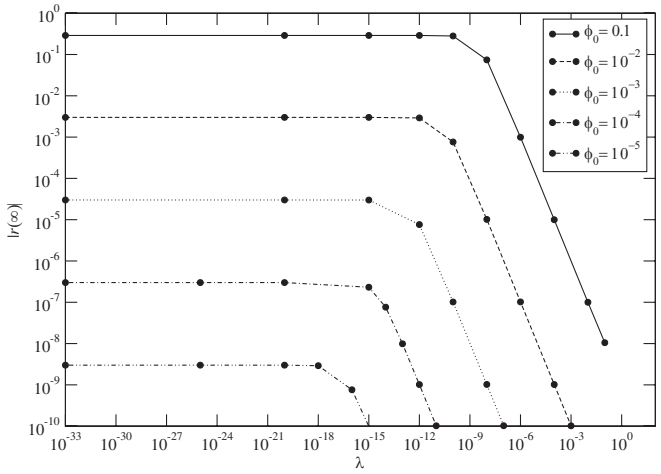

FIG. 5. Ratio of the baryon to particle number density at large times for various initial values of Φ_0 and couplings λ.

equal ϕ_0 contours, where $\phi_0 = \sqrt{\lambda}\Phi_0/m_\Phi$. For a given contour, the saturation value for small values of λ is given by the classical result, $|r(\infty)| \approx 10\phi_0^2$, which corresponds to the horizontal part of the curve. When λ becomes larger than about $10^{-6}\phi_0^2$, the nonequilibrium effects start to operate and significantly diminish the saturation ratio. For a wide range of parameters, this can result in r saturating toward the observed value of the baryon asymmetry, as shown by the right end-points of the contours.

As an illustration, let us recall the sample values of the model parameters cited after Eq. (6), which corresponds to the left end of the $\phi_0 = 10^{-2}$ contour in Fig. 5. Now let us entertain the possibility that the supersymmetry-breaking scale may be as high as the grand unification scale, i.e., $M_S \lesssim M_G$. We then find $\lambda \lesssim 10^{-3}$ and the baryon asymmetry is reduced by the nonequilibrium dynamics to the present observed value, $|r(\infty)| \approx 10^{-10}$, corresponding to the right end of the $\phi_0 = 10^{-2}$ contour in Fig. 5.

VII. CONCLUSIONS

We have studied the effects of nonequilibrium dynamics in the Affleck-Dine mechanism of baryogensis. Within the context of the model (2), we find that, for very weak couplings, the ratio of the baryon to particle number density is approximately $10\lambda\Phi_0^2/m_\Phi^2$, as dictated by the classical dynamics, but for larger couplings it is driven by the nonequilibrium effects toward a smaller value given by $|r| \approx 10^{-5}\lambda\Phi_0^4/m_\Phi^4$. Interestingly, in some cases these nonequilibrium effects can reduce the baryon asymmetry generated in the classical Affleck-Dine mechansim to the present observed value without having recourse to additional dilution processes. This encouraging result suggests that nonequilibrium dynamics can play a significant role in the evolution of the early Universe. It is therefore important to explore other possible manifestations of these nonequilibrium effects. The methodology developed and presented in this paper will be useful for such studies.

ACKNOWLEDGMENTS

This work was supported in part by the National Science Council, ROC, under grant NSC92-2112-M-001-029 (NSC93-2112-M-259-007) as well as the short-term visiting program of the Royal Society, and in part by the U. S. Department of Energy under grant DE-FG02-84ER40163. C. N. L. would like to thank the members of the Institute of Physics at the Academia Sinica in Taipei, Taiwan, especially H.-Y. Cheng, C.-Y. Cheung, S.-P. Li, and K.-W. Ng, for their hospitality. He also thanks S.-Y. Wang for a useful discussion.

[1] A. G. Cohen, A. De Rujula, and S. L. Glashow, Astrophys. J. **495**, 539 (1998).
[2] B. Fields and S. Sarkar, Phys. Lett. B **592**, 1 (2004).
[3] For a review, see K. Enqvist and A. Mazumdar, Phys. Rep. **380**, 99 (2003).
[4] I. Affleck and M. Dine, Nucl. Phys. **B249**, 361 (1985).
[5] A. D. Linde, Phys. Lett. B **160**, 243 (1985); J. Ellis *et al.*, Phys. Lett. B **191**, 343 (1987).
[6] K. Enqvist, K.-W. Ng, and K. A. Olive, Phys. Rev. D **37**, 2111 (1988).
[7] A. D. Dolgov *et al.*, Phys. Rev. D **67**, 103515 (2003).
[8] K.-W. Ng, Nucl. Phys. **B321**, 528 (1989); M. Dine, L. Randall, and S. Thomas, Nucl. Phys. **B458**, 291 (1996).
[9] D. Boyanovsky, D.-S. Lee, and A. Singh, Phys. Rev. D **48**, 800 (1993); D. Boyanovsky, H. J. de Vega, R. Holman, D.-S. Lee, and A. Singh *ibid.* **51**, 4419 (1995); D. Boyanovsky, M. D'Attanasio, H. J. de Vega, R. Holman, and D.-S. Lee*ibid.* **52**, 6805 (1995); D. Boyanovsky, I. D. Lawrie, and D.-S. Lee *ibid.* **54**, 4013 (1996).
[10] E. Calzetta and B. L. Hu, Phys. Rev. D **35**, 495 (1987); **37**, 2878 (1988); **52**, 6770 (1995); B. L. Hu, Physica A (Amsterdam) **158**, 399 (1989).
[11] F. Cooper, S. Habib, Y. Kluger, E. Mottola, J. P. Paz, and P. R. Anderson, Phys. Rev. D **50**, 2848 (1994); F. Cooper, Y. Kluger, E. Mottola, and J. P. Paz *ibid.* **51**, 2377 (1995); F. Cooper, S. Habib, Y. Kluger, and E. Mottola *ibid.* **55**, 6471 (1997).
[12] Y.-Y. Charng, K.-W. Ng, C.-Y. Lin, and D.-S. Lee, Phys. Lett. B **548**, 175 (2002); W.-L. Lee, Y.-Y. Charng, D.-S. Lee, and L.-Z. Fang, Phys. Rev. D **69**, 123522 (2004).
[13] J. Schwinger, J. Math. Phys. (N.Y.) **2**, 407 (1961); L. V. Keldysh, Sov. Phys. JETP **20**, 1018 (1965); K. T. Mahanthappa, Phys. Rev. **126**, 329 (1962); P. M. Bakshi and K. T. Mahanthappa, J. Math. Phys. (N.Y.) **4**, 1 (1963);

4, 12 (1963); K.-C. Chou, Z.-B. Su, B.-L. Hao, and L. Yu, Phys. Rep. **118**, 1 (1985); J. Rammer and H. Smith, Rev. Mod. Phys. **58**, 323 (1986).

[14] M. Le Bellac, *Thermal Field Theory* (Cambridge University Press, Cambridge, England, 1996).

[15] L. Kofman, A. D. Linde, and A. A. Starobinsky, Phys. Rev. Lett. **73**, 3195 (1994); L. Kofman, A. D. Linde, A. A. Starobinsky, Phys. Rev. D **56**, 3258 (1997); Y. Shtanov, J. Traschen, and R. Brandenberger, Phys. Rev. D **51**, 5438 (1995); D.-S. Lee and K.-W. Ng, Phys. Rev. D **61**, 085003 (2000).